COMMUNICATION

Atomic layer deposited $Li_4Ti_5O_{12}$ on nitrogen-doped carbon nanotubes†

Xiangbo Meng, Jian Liu, Xifei Li, Mohammad Norouzi Banis, Jinli Yang, Ruying Li and Xueliang Sun*

Atomic layer deposition was used for the synthesis of ternary spinel $Li_4Ti_5O_{12}$ compounds on nitrogen-doped carbon nanotubes, featuring its accurate tunability of elemental compositions.

The quest for alternative energy sources is urgent while fossil fuels as our main sources are depleting and causing a series of environmental issues. Among the potential alternatives, lithium-ion batteries (LIBs) are the most promising.[1,2] For next-generation use in hybrid or pure electric vehicles (HEVs, or EVs), however, LIBs require new materials to address the current issues in energy density, safety, cost and service-life.[3–6] $Li_4Ti_5O_{12}$ (LTO) is an attractive anode material, offering LIBs with reliable safety, having negligible volume change, no electrolyte decomposition and no formation of a solid electrolyte interphase.[3,7,8] Consequently, many efforts were conducted for developing LTO and its composites, including sol–gel,[9–11] solid-state,[12,13] cellulose-assisted combustion,[13–15] microwave,[16] hydrothermal,[17] solvothermal,[18] spray pyrolysis,[19] and molten salt processes.[20]

In this work, we report the first attempt in synthesizing nanostructured $Li_4Ti_5O_{12}$ using atomic layer deposition (ALD), demonstrating that ALD enables the precise control of elemental compositions and shows exceptional flexibility. As a thin film deposition method for semiconductor manufacturing, only in the past decade was ALD recognized as a route for new nanostructured materials,[21–24] featuring its advantages in atomic-scale control, excellent uniformity and conformality and low deposition temperature. ALD has achieved extensive successes for metals, binary oxides and even organic polymers.[23,25] Recently, there has been an increasing interest in ALD for developing ternary or more complicated compounds[26,27] and the thrust mainly lies in the fine-tunability of ALD in the composition of compounds. In this work, we present our successful fabrication of the nanocomposites of $Li_4Ti_5O_{12}$ based on nitrogen-doped carbon nanotubes (N-CNTs)

and have paved a new route for developing ternary LTO nanocomposites using ALD.

N-CNTs have proved their exceptional physical properties, ascribed to the doped-N atoms. The N-CNTs in this study were grown *via* chemical vapor deposition (CVD) and their N contents were around 8.4 at.%, as detailed in our earlier work.[28] The N-CNTs could facilitate ALD *via* their N-related defects.[29] The ALD-$Li_4Ti_5O_{12}$ process in this work was performed through combining two sub-ALD systems, *i.e.*, Ti–O from titanium isopropoxide (TTIP, $Ti(OCH(CH_3)_2)_4$) and deionized water,[30,31] and Li–O from $Li(O^tBu)$ and deionized water.[32] Through tuning the ratio between Ti–O and Li–O to an optimal value *via* adjusting their ALD cycles, we deposited an amorphous Li–Ti–O compound on N-CNTs and the compound was transformed to the crystalline $Li_4Ti_5O_{12}$ by annealing. We found that the desirable ratio for the sub-ALD systems (*i.e.*, Ti–O : Li–O) was 5 : 4, in terms of their ALD cycles. Apparently, the ALD-$Li_4Ti_5O_{12}$ process is a stoichiometric route for fabricating the $Li_4Ti_5O_{12}$ compound, as schematically illustrated in Scheme 1.

In the ALD-$Li_4Ti_5O_{12}$ process, the N-CNTs grown on carbon papers (Fig. ESI-1 in the ESI†) were first loaded into a commercial ALD reactor (Savannah 100, Cambridge Nanotechnology Inc., USA) preheated to a certain temperature which was set at 250 °C in this work. Then, the two sub-ALD systems were run one by one, as illustrated by Scheme 1. After 5 cycles of the sub-ALD of Ti–O, 4 cycles of the sub-ALD of Li–O followed. The two sub-ALD systems ran in an alternating manner. For the sub-ALD of Ti–O, TTIP was heated to 70 °C while water was kept at room temperature in order to provide sufficient vapors. The procedures for the sub-ALD of Ti–O were set as follows: (1) a 1.0 s supply of TTIP; (2) a 3.0 s extended exposure of TTIP to the N-CNTs; (3) a 10.0 s purge of oversupplied TTIP and any by-products; (4) a 2.0 s supply of water vapor; (5) a 3.0 s extended exposure of water vapor to N-CNTs; (6) a 10.0 s purge of oversupplied water and any by-products. The aforementioned six-step sequence constituted one sub-ALD cycle of Ti–O. The sub-ALD of Li–O took the same procedures as the sub-ALD of Ti–O, except for a preheated temperature of 170 °C for $Li(O^tBu)$. Thus, a 5-cycle Ti–O and 4-cycle Li–O constituted one ALD cycle of Li–Ti–O. Additionally, the delivery lines were heated to 200 °C in

Department of Mechanical and Materials Engineering, The University of Western Ontario, London, ON N6A 5B8, Canada. E-mail: xsun@eng.uwo.ca

† Electronic supplementary information (ESI) available: XRD patterns for pristine N-CNTs and Li–Ti–O coated N-CNTs, $Li_4Ti_5O_{12}$ composites annealed at 850 and 950 °C, and rutile TiO_2 adhered on N-CNTs as an impurity. See DOI: 10.1039/c3ra00033h
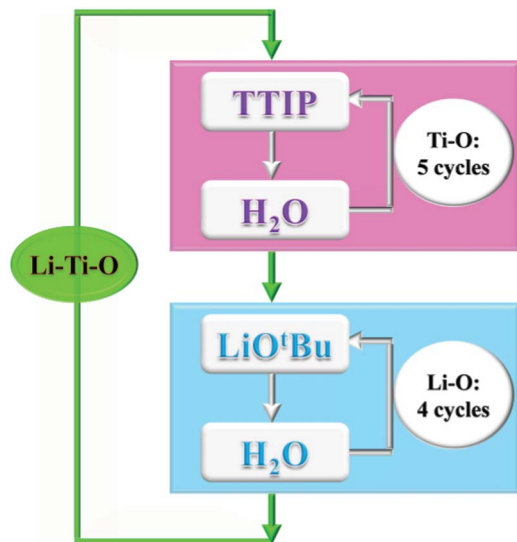
Scheme 1 Schematic illustration of the ALD of Li–Ti–O compound.

order to prevent the precursors from condensing. Nitrogen was used as the carrier gas with a flow rate of 20 sccm and the ALD reactor was sustained at a low level of pressure (typically 0.4 Torr) with a vacuum pump (Pascal 2005 I, Adixon).

The ALD coatings of Li–Ti–O on N-CNTs were observed using field emission scanning electron microscopy (FE-SEM, Hitachi 4800 S) and transmission electron microscopy (TEM, JEOL 2010 FEG), as shown in Fig. 1. In comparison with the pristine N-CNTs (Fig. 1(a)), the ALD-coatings of Li–Ti–O enlarged the diameters of N-CNTs after 20 (Fig. 1(b)) and 30 (Fig. 1(c)) cycles. It is worth noting that the Li–Ti–O coatings on N-CNTs were uniform and conformal. The TEM image (Fig. 1(d)) revealed that the Li–Ti–O coating was a uniform thickness of around 22 nm after 40 cycles. Thus, the Li–Ti–O coating accounted for an average deposition rate of 5.5 Å/cycle. By itself, ALD-TiO_2 could produce a growth rate

Fig. 1 SEM images of (a) pristine N-CNTs and (b,c) ALD Li–Ti–O coated N-CNTs by (b) 20 and (c) 30 cycles; (d) TEM image of 40-cycle ALD Li–Ti–O coated N-CNTs.

of 0.4 Å/cycle on CNTs at 250 °C.[31] ALD-LiOH was reported with a growth rate of 12.7 ng cm^{-2}/cycle,[32] standing for a growth rate of 0.87 Å/cycle. Consequently, the combination of 5 individual sub-cycles of Ti–O and 4 individual sub-cycles of Li–O offers a growth rate of 5.48 Å/cycle, very consistent with our observation of 5.5 Å/cycle for the Li–Ti–O compound. In other words, the combined ALD for the Li–Ti–O compound showed little change in its growth rate with respect to the addition of individual Li–O and Ti–O sub-cycles. A further evaluation revealed that the resultant Li : Ti ratio is 2.0. The characterization of X-ray diffraction (XRD, Inel multi-purpose diffractometer) revealed the amorphous nature of the Li–Ti–O coating (see Fig. ESI-1 in the ESI†), and there was no evident difference observed from the XRD patterns before and after Li–Ti–O coating.

To confirm that the ALD route enabled the synthesis of the spinel $Li_4Ti_5O_{12}$ through precisely controlling elemental compositions, we annealed the 40-cycle Li–Ti–O coated N-CNTs under two high temperatures, 850 and 950 °C in Ar. The received composites were characterized by XRD, as shown in Fig. 2. Besides the two peaks of graphite (002) and (004) (JCPDS PDF No. 41-1487) from the N-CNTs, the two annealed samples additionally disclosed a series of strong peaks being characteristic of spinel $Li_4Ti_5O_{12}$ (JCPDS PDF No. 49-0207) as well as several weak peaks for rutile TiO_2 (JCPDS PDF No. 04-0551). Obviously, the ALD route was successful for synthesizing the ternary spinel $Li_4Ti_5O_{12}$ compound in a controllable manner. The effects of the two annealing temperatures on XRD patterns were comparable. We further examined the morphological changes due to the annealing effects, as shown in Fig. 3 and Fig. ESI-2 in the ESI.† Fig. 3(a) and (c) reveal that the uniform and conformal Li–Ti–O coatings changed into bean-like $Li_4Ti_5O_{12}$ nanoparticles chained by N-CNTs after 3 h annealing at 850 °C. In comparison, Fig. 3(b) and (d) disclose that
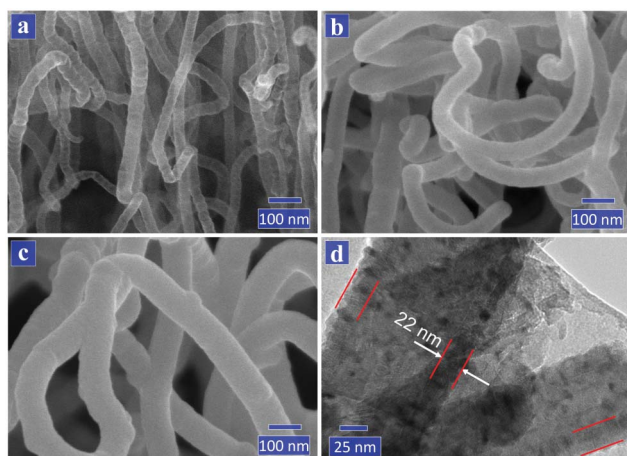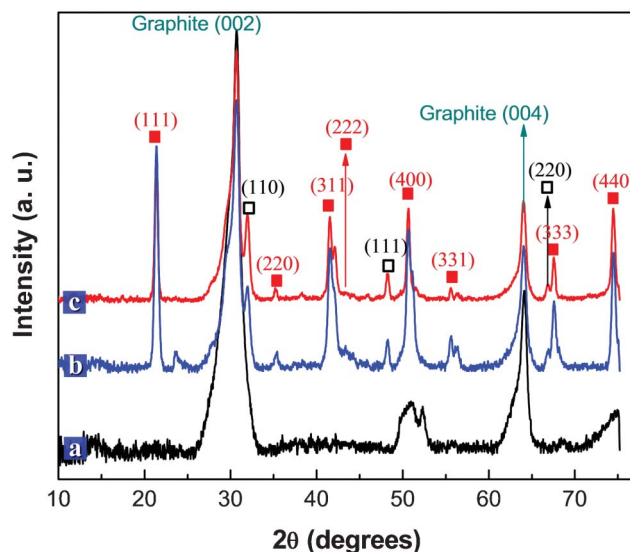
Fig. 2 XRD patterns for the ALD of Li–Ti–O of 40 cycles. (a) The as-deposited sample in addition to the annealed samples at (b) 850 and (c) 950 °C for 3 h in Ar. (■) identifies the peaks of the spinel $Li_4Ti_5O_{12}$ and (□) signifies the peaks of the rutile TiO_2.
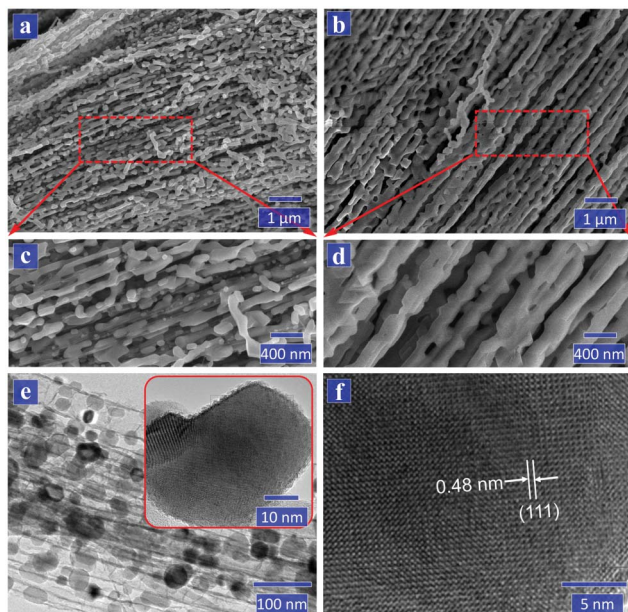
Fig. 3 Morphological and structural characteristics of the annealed Li–Ti–O coatings: SEM images of the sample annealed at (a, c) 850 and (b, d) 950 °C, (e) TEM images of the sample annealed at 850 °C (inset: a crystalline nanoparticle), and (f) HR-TEM image of a local area of the nanoparticle in the inset.

a higher annealing temperature of 950 °C produced more integral networks of $Li_4Ti_5O_{12}$ supported by N-CNTs. The morphological changes due to the annealing effects at different temperatures were probably due to different reaction rates between the Li–O and Ti–O component. Further examination with high-resolution TEM (HR-TEM, JEOL 2010 FEG) is shown in Fig. 3(e) and (f). The HR-TEM image in Fig. 3(f) clearly reveal the characteristic lattices of (111) planes of spinel $Li_4Ti_5O_{12}$. We also observed a few rutile TiO_2 nanoparticles as impurities in the N-CNT-supported $Li_4Ti_5O_{12}$ composites, as shown in Fig. ESI-3 in the ESI.† Based on the information from the XRD patterns in Fig. 2 and our HR-TEM observation, we propose that the TiO_2 impurity is secondary to the spinel $Li_4Ti_5O_{12}$ and in a trace amount in the received compound. It is worth noting that the Li : Ti ratio in $Li_4Ti_5O_{12}$ is 0.8, far less than the Li : Ti ratio of 2.0 in the ALD-deposited Li–Ti–O amorphous compound. Thus, it is reasonable to conclude that there was much Li loss in the annealing process. The reason lies in the vaporization of Li–O[33,34] during the annealing process. The most recent effort[35] for ALD-$Li_xTi_yO_z$ claimed the success of $Li_4Ti_5O_{12}$ after annealing 110 nm thick films in N_2. The authors deposited the films on Pt-coated Si wafers with a 2 : 3 cycle ratio of Li–O : Ti–O, accounting for a Li : Ti ratio of 1.5. However, their XRD peaks for $Li_4Ti_5O_{12}$ were too weak and little, in contrast with the peaks from substrates. In comparison, our XRD patterns and TEM showed more evidence for $Li_4Ti_5O_{12}$. The main difference lies in a higher Li : Ti ratio used in our study, being advantageous for mitigating Li loss. Even so, in the future it deserves a further improvement on the $Li_4Ti_5O_{12}$ synthesis. In this way, annealing a Li–Ti–O compound in a sealed container may help reduce Li loss and thereby produce pure $Li_4Ti_5O_{12}$ compound from Li–Ti–O

compounds with a Li : Ti ratio close to 0.8. In addition, the use of Ar is important in this study. Besides protecting N-CNTs from oxidation, Ar might also have mitigated the vaporization of Li–O during annealing.

In summary, this work has demonstrated that ALD is viable for developing ternary spinel $Li_4Ti_5O_{12}$ nanostructured composites. This method features its precise control of elemental compositions of $Li_4Ti_5O_{12}$. We expect that more interest will be inspired by this timely report on ALD-$Li_4Ti_5O_{12}$ and our further efforts will be on investigating the performance of the synthesized N-CNT–$Li_4Ti_5O_{12}$ composites as battery anodes and on other complicated battery compounds, especially lithium metal oxides as battery cathodes.

Notes and references

1 L.-X. Yuan, Z.-H. Wang, W.-X. Zhang, X.-L. Hu, J.-T. Chen, Y.-H. Huang and J. B. Goodenough, *Energy Environ. Sci.*, 2011, **4**, 269–284.
2 M. R. Palacín, *Chem. Soc. Rev.*, 2009, **38**, 2565–2575.
3 B. Scrosati and J. Garche, *J. Power Sources*, 2010, **195**, 2419–2430.
4 J. B. Goodenough and Y. Kim, *Chem. Mater.*, 2010, **22**, 587–603.
5 P. Arora, R. E. White and M. Doyle, *J. Electrochem. Soc.*, 1998, **145**, 3647–3667.
6 P. Verma, P. Maire and P. Novák, *Electrochim. Acta*, 2010, **55**, 6332–6341.
7 Z. Yang, J. Zhang, M. C. W. Kintner-Meyer, X. Lu, D. Choi, J. P. Lemmon and J. Liu, *Chem. Rev.*, 2011, **111**, 3577–3613.
8 D. Deng, M. G. Kim, J. Y. Lee and J. Cho, *Energy Environ. Sci.*, 2009, **2**, 818–837.
9 N. A. Alias, M. Z. Kufian, L. P. Teo, S. R. Majid and A. K. Arof, *J. Alloys Compd.*, 2009, **486**, 645–648.
10 Z.-Q. He, L.-Z. Xiong, S. Chen, X.-M. Wu, W.-P. Liu and K.-L. Huang, *Trans. Nonferrous Met. Soc. China*, 2010, **20**, s262–s266.
11 K. Naoi, S. Ishimoto, Y. Isobe and S. Aoyagi, *J. Power Sources*, 2010, **195**, 6250–6254.
12 X. Li, M. Qu and Z. Yu, *Solid State Ionics*, 2010, **181**, 635–639.
13 T. Yuan, R. Cai, R. Ran, Y. Zhou and Z. Shao, *J. Alloys Compd.*, 2010, **505**, 367–373.
14 T. Yuan, R. Cai, P. Gu and Z. Shao, *J. Power Sources*, 2010, **195**, 2882–2887.
15 T. Yuan, X. Yu, R. Cai, Y. Zhou and Z. Shao, *J. Power Sources*, 2010, **195**, 4997–5004.
16 L. H. Yang, C. Dong and J. Guo, *J. Power Sources*, 2008, **175**, 575–580.
17 J. Chen, L. Yang, S. Fang and Y. Tang, *Electrochim. Acta*, 2010, **55**, 6596–6600.
18 D. K. Lee, H.-W. Shim, J. S. An, C. M. Cho, I.-S. Cho, K. S. Hong and D.-W. Kim, *Nanoscale Res. Lett.*, 2010, **5**, 1585–1589.
19 S. H. Ju and Y. C. Kang, *J. Power Sources*, 2010, **195**, 4327–4331.
20 M. M. Rahman, J.-Z. Wang, M. F. Hassan, S. Chou, D. Wexler and H.-K. Liu, *J. Power Sources*, 2010, **195**, 4297–4303.

21 M. Knez, K. Nielsch and L. Niinistö, *Adv. Mater.*, 2007, **19**, 3425–3438.

22 H. Kim, H.-B.-R. Lee and W.-J. Maeng, *Thin Solid Films*, 2009, **517**, 2563–2580.

23 S. M. George, *Chem. Rev.*, 2010, **110**, 111–131.

24 X. Meng, X.-Q. Yang and X. Sun, *Adv. Mater.*, 2012, **24**, 3589–3615.

25 R. L. Puurunen, *J. Appl. Phys.*, 2005, **97**, 121301.

26 M. Putkonen, T. Aaltonen, M. Alnes, T. Sajavaara, O. Nilsen and H. Fjellvåg, *J. Mater. Chem.*, 2009, **19**, 8767–8771.

27 T. Aaltonen, M. Alnes, O. Nisen, L. Costelle and H. Fjellvåg, *J. Mater. Chem.*, 2010, **20**, 2877–2881.

28 H. Liu, Y. Zhang, R. Li, X. Sun, S. Désilets, H. Abou-Rachid, M. Jaidann and L.-S. Lussier, *Carbon*, 2010, **48**, 1498–1507.

29 X. Meng, Y. Zhong, Y. Sun, M. N. Banis, R. Li and X. Sun, *Carbon*, 2011, **49**, 1133–1144.

30 X. Meng, D. Geng, J. Liu, R. Li and X. Sun, *Nanotechnology*, 2011, **22**, 165602.

31 X. Meng, M. N. Banis, D. Geng, X. Li, Y. Zhang, R. Li, H. Abou-Rachid and X. Sun, *Appl. Surf. Sci.*, 2013, **266**, 132–140.

32 A. S. Cavanagh, Y. Lee, B. Yoon and S. M. George, *ECS Transactions*, 2010, **33**, 223–229.

33 T. Sata, *Ceram. Int.*, 1998, **24**, 53–59.

34 E. McCalla, G. H. Carey and J. R. Dahn, *Solid State Ionics*, 2012, **219**, 11–19.

35 V. Miikkulainen, O. Nilsen, M. Laitinen, T. Sajavaara and H. Fjellvåg, *RSC Advances*, DOI: 10.1039/C3RA40745D.